ARTICLE

Linear and Nonlinear Spectra in Photosynthetic Light Harvesting Complexes: Benchmark Tests of Modified Redfield Method†

Yuan-yuan Jing, Kai Song, Shu-ming Bai, Qiang Shi*

Beijing National Laboratory for Molecular Sciences, State Key Laboratory for Structural Chemistry of Unstable and Stable Species, Institute of Chemistry, Chinese Academy of Sciences, Beijing 100190, China

(Dated: Received on June 17, 2015; Accepted on July 13, 2015)

We employ the numerically exact hierarchical equations of motion (HEOM) method to perform benchmark tests for the popular modified Redfield method in calculating linear and nonlinear spectroscopic signals of molecular aggregates in photosynthetic light harvesting complexes. It is currently well known that the perturbative and Markovian approximations involved in the modified Redfield equation may give inappropriate description of the excitation energy transfer processes in the intermediate coupling regime. An interesting topic is thus to test the validity of the modified Redfield method in calculating various types of spectroscopic signals. By using model dimers with different sets of parameters and a model of the Fenna-Matthews-Olson complex, we calculate and compare the absorption, emission, and 2D spectra using the modified Redfield and HEOM methods. It is found that results from the modified Redfield method agree well with the HEOM ones in a wide range of parameter regimes. The comparison also helps to understand the quantum beating signals in the 2D spectra of the photosynthetic light harvesting complexes.

Key words: Linear spectra, Nonlinear spectra, Light harvesting complexes, Modified Redfield method

I. INTRODUCTION

Various types of molecular aggregates are ubiquitous in natural and artificial systems [1−4]. The molecular aggregates in photosynthetic light harvesting systems are crucial for absorbing and transferring the solar energy to the reaction center for further chemical reactions [2, 3]. As linear and nonlinear spectroscopic experiments are important tools to investigate the structure and dynamics in molecular aggregates, theory and simulation play a key role in explaining the experimental spectra and extracting important structural and dynamical information [5−7]. For example, the recent observation of long time quantum coherence in the two-dimensional (2D) spectra in photosynthetic light harvesting complexes [8−14], have initialized a wide discussion on their origins and the roles of the pigment-protein interaction, and a full understanding of these important problems requires accurate theoretical modeling of the excitation energy transfer dynamics and related spectroscopic signals.

For the molecular aggregates in photosynthetic light harvesting complexes, two different types of interactions are important to determine the dynamics and spectroscopic properties: the intermolecular electronic coupling between neighbour molecules and the electron-vibrational coupling between the electronic transition and the vibrational degrees of freedom. When one type of interaction is significantly larger than the other, approximate methods can be used to calculate the dynamics and spectroscopic signals. For example, if the intermolecular electronic coupling is weak, the Fermi's golden rule (FGR) [15] can be used. On the other hand, if the electron-vibrational coupling is weak, the second order generalized quantum master equations (GQMEs) can be employed [16−18]. But in the case of intermediate coupling regime where the two different types of couplings are of similar strength, the above methods often become invalid [7, 19]. In previous work, we have employed the hierarchical equations of motion (HEOM) method to calculate the dynamics and spectroscopic signals of molecular aggregates in the intermediate coupling regime, and examined the applicability of many approximate methods [20−23].

In this work, we compare results from the popular modified Redfield method with numerically exact results from the HEOM method in calculating of the linear and nonlinear spectroscopic signals. The standard Redfield theory is an important method in simulating reduce dynamics of a quantum system coupled to a dissipative bath [24, 25]. It treats the system-bath interactions in the excitonic basis using second

†Dedicated to Professor Qing-shi Zhu on the occasion of his 70th birthday.

*Author to whom correspondence should be addressed. E-mail: qshi@iccas.ac.cn

order perturbation and Markovian approximation [24, 25]. The Markovian approximation in the standard Redfield theory has many drawbacks in calculations of spectroscopic signals. Mukamel and coworkers first introduced the modified Redfield method to calculate the nonlinear optical response functions [26], where the diagonal system-bath interactions in the excitonic basis are treated exactly using analytical expressions, and the off-diagonal terms are treated perturbatively with the Markovian approximation as in the standard Redfield theory. Later, Fleming and coworkers [27], Renger and Marcus [28], developed similar approaches to calculate the optical lineshapes for molecular aggregates. The modified Redfield method has since been widely used in calculating population dynamics, absorption, emission, pump-probe and 2D spectra [29−32].

There are several advantages of the modified Redfield theory in calculating the linear and nonlinear spectroscopic signals: (i) Since the modified Redfield method employs the excitonic basis, the spectroscopic signals can be easily decomposed into contributions from each exciton states. This is especially useful when the intermolecular electronic coupling is relatively strong, and the exciton states are well defined. (ii) The modified Redfield method allows to treat easily with large molecular aggregates and complex spectral densities, where the more accurate methods like the HEOM approach are still less efficient due to the high computational costs. However, the perturbative and Markovian approximations employed in deriving the modified Redfield equation have been found to have many problems in calculating the excitation energy transfer dynamics in the intermediate coupling regimes [7, 19]. Another disadvantage of the modified Redfield method is that, the neglect of coherent dynamics (in the excitonic basis) also makes it impossible to study correctly the effect of coherent population dynamics. Although several new corrections to the modified Redfield method have recently been proposed to improve its capability [33−36], it is still very interesting to test the applicability of the modified Redfield method in calculating various types of spectroscopic signals in different parameter regimes.

In this work, the Frenkel exciton model of molecular aggregates in photosynthetic light harvesting complexes, and equations to calculate various types of spectroscopic signals based on the modified Redfield method are presented. The results of absorption and emission line shapes, as well as two-dimensional spectra calculated by the modified Redfield method are compared with the numerically exact results from the HEOM calculations.

II. THEORY

A. The Frenkel exciton model

To study the spectroscopic signals of the molecular aggregate, we consider a Frenkel exciton model of N two-level molecules coupled to a phonon bath, where the total Hamiltonian is written as,

$$H = H_{\rm e} + H_{\rm ph} + H_{\text{e-ph}} \tag{1}$$

here, the excitonic Hamiltonian $H_{\rm e}$ describes the electronic degrees of freedom,

$$H_{\rm e} = \sum_{m=1}^{N} \epsilon_m a_m^+ a_m + \sum_{m=1}^{N} \sum_{n<m} J_{mn}(a_m^+ a_n + a_n^+ a_m) \tag{2}$$

where ϵ_m is the transition energy on the mth molecule, a_m^+ and a_m are the creation and annihilation operators of the electronic transition on the mth molecule, and J_{mn} is the intermolecular electronic coupling. The intermolecular coupling J_{mn} is assumed to be independent of the nuclear degrees of freedom.

It is assumed that the electronic excitation on the mth molecule couples independently to its own vibrational degrees of freedom. The phonon (vibrational) Hamiltonian $H_{\rm ph}$ is given by

$$H_{\rm ph} = \sum_{m=1}^{N} \sum_{j=1}^{N_b^m} \frac{1}{2} \left(p_{mj}^2 + \omega_{mj}^2 x_{mj}^2 \right) \tag{3}$$

where N_b^m is the number of vibrational modes belonging to molecule m, x_{mj} and p_{mj} are the position and momentum of the jth harmonic oscillator bath mode with frequency ω_{mj}.

The electron-phonon coupling $H_{\text{e-ph}}$ is assumed to cause only electronic energy fluctuations that are independent for each chromophore. $H_{\text{e-ph}}$ is also assumed to be linear in the bath coordinates, such that

$$\begin{aligned} H_{\text{e-ph}} &= \sum_{m=1}^{N} \sum_{j=1}^{N_b^m} c_{mj} x_{mj} a_m^+ a_m \\ &= \sum_{m=1}^{N} F_m a_m^+ a_m \end{aligned} \tag{4}$$

where the collective bath coordinate F_m is defined as $F_m = \sum_{j=1}^{N_b^m} c_{mj} x_{mj}$.

The spectral density $J_m(\omega)$ is used to characterize electron-phonon interaction on the mth molecule, which is defined as

$$J_m(\omega) = \frac{\pi}{2} \sum_{j=1}^{N_b^m} \frac{c_{mj}^2}{\omega_{mj}} \delta(\omega - \omega_{mj}) \tag{5}$$

For simplicity, we use the same spectral density $J(\omega)$ for all molecules in the aggregate, and assume $\hbar$=1 throughout this work.

The HEOM approach [37–42] is a non-perturbative method that can be used to study the excitation energy transfer dynamics and related spectroscopic signals in

DOI:10.1063/1674-0068/28/cjcp1506126

the intermediate coupling regime [19–23, 43–45]. In the past few years, we have applied the HEOM approach in calculating the absorption and emission line shapes [20, 23], and the 2D spectra [21, 22]. The HEOM approach is employed to generate the numerically exact results used in this work, and the computation details of various types of spectroscopic signals can be found in our previous works [20–23].

B. The modified Redfield method to calculate spectroscopic signals

In the modified Redfield formalism, the system Hamiltonian is first diagonalized to obtain the exciton eigenstates, and the total Hamiltonian is divided into two parts:

$$H = H_0 + H' \tag{6}$$

where H_0 and H' represent a reference part and a perturbation part, respectively:

$$H_0 = H_{\rm S} + H_{\rm B} + \sum_{\mu} |\mu\rangle\langle\mu|H_{\rm SB}|\mu\rangle\langle\mu| \tag{7}$$

$$H' = \sum_{\mu\nu,\mu\neq\nu} |\mu\rangle\langle\mu|H_{\rm SB}|\nu\rangle\langle\nu| \tag{8}$$

where $|\mu\rangle$ and $|\nu\rangle$ are exciton eigenstates of the electronic degrees of freedom.

The H_0 part containing the system, bath, and diagonal part of the system-bath interaction is treated nonperturbatively, while the H' part containing the off-diagonal system-bath coupling is treated using second order perturbation and the Markovian approximation [26]. In the following subsections, we will not get into details regarding the derivation of the modified Redfield equations, but instead, present only the equations used to calculate the linear and nonlinear spectroscopic signals in the modified Redfield method.

1. Population transfer rates

In calculating different types of spectroscopic signals, population transfer rate from exciton state $|\mu\rangle$ to state $|\nu\rangle$ is needed. When assuming that all monomers in the molecular aggregate have the same spectral densities, the population transfer rate between different exciton states can be calculated as [26, 27, 46],

$$k_{\mu\to\nu} = \int_{-\infty}^{+\infty} {\rm d}t \exp(i\omega_{\mu\nu}t) \exp[\phi_{\mu\nu}(t) - \phi_{\mu\nu}(0)]\{[\lambda_{\mu\nu} + G_{\mu\nu}(t)]^2 + F_{\mu\nu}(t)\} \tag{9}$$

where $\omega_{\mu\nu}$=ε_μ−ε_ν is the energy difference between the exciton eigenstates μ and ν, and the time-dependent functions ϕ, G, and F are given by

$$\phi_{\mu\nu}(t) = \sum_i (|c_i^\mu|^2 - |c_i^\nu|^2)^2 \phi_0(t) \tag{10}$$

$$G_{\mu\nu}(t) = \sum_i \left[(c_i^\mu)^3 c_i^\nu - (c_i^\nu)^3 c_i^\mu\right] \phi_1(t) \tag{11}$$

$$F_{\mu\nu}(t) = \sum_i |c_i^\mu|^2 |c_i^\nu|^2 \phi_2(t) \tag{12}$$

$$\phi_1(t) = \frac{1}{\pi}\int_0^\infty {\rm d}\omega J(\omega)\omega^{-1}\Big[\cos(\omega t) - i\coth\left(\frac{1}{2}\omega\beta\right)\sin(\omega t)\Big] \tag{13}$$

and for n=0, 2,

$$\phi_n(t) = \frac{1}{\pi}\int_0^\infty {\rm d}\omega J(\omega)\omega^{n-2}\Big[\coth\left(\frac{1}{2}\omega\beta\right)\cdot \cos(\omega t) - i\sin(\omega t)\Big] \tag{14}$$

where β=$1/kT$, k is the Boltzmann constant and T is the temperature. In Eqs.(10)−(12), c_i^μ is the coefficient of the exciton eigenstate $|\mu\rangle$ in the ith site basis. We also note that Eq.(13) and Eq.(14) are slightly different from those in Ref.[46], because a different definition of the spectral density $J(\omega)$ is used.

The time-independent term $\lambda_{\mu\nu}$ in Eq.(9) is defined as:

$$\lambda_{\mu\nu} = \sum_i \left[(c_i^\mu)^3 c_i^\nu + (c_i^\nu)^3 c_i^\mu\right] E_\lambda \tag{15}$$

where the reorganization energy E_λ is calculated as

$$E_\lambda = \frac{1}{\pi}\int_0^\infty {\rm d}\omega \frac{J(\omega)}{\omega} \tag{16}$$

2. Absorption and emission line shapes

In the modified Redfield method, the absorption and emission line shapes can be expressed as the summation of the contribution from all the exciton states [26–29],

$$I_{\rm abs}(\omega) \propto \sum_\mu |d_\mu|^2 D_\mu(\omega) \tag{17}$$

$$I_{\rm ems}(\omega) \propto \sum_\mu \frac{\exp(-\omega_{\mu 0}/kT)}{\sum_\nu \exp(-\omega_{\nu 0}/kT)} |d_\mu|^2 D'_\mu(\omega) \tag{18}$$

In Eq.(17) and Eq.(18), d_μ is transition dipole in the excitonic basis, $\omega_{\mu 0}$ is the transition energy from the ground state to the exciton eigenstate $|\mu\rangle$. The line shape function $D_\mu(\omega)$ for absorption is obtained from

$$D_\mu(\omega) = {\rm Re}\int_0^\infty {\rm d}t \exp[i(\omega - \omega_{\mu 0} - \gamma_{\mu\mu}E_\lambda)t]\cdot \exp[G_\mu(t) - G_\mu(0)] \exp\left(-\frac{t}{\tau_\mu}\right) \tag{19}$$

DOI:10.1063/1674-0068/28/cjcp1506126

and $D'_\mu(\omega)$ for the emission line shape is give by

$$D'_\mu(\omega) = \mathrm{Re}\int_0^\infty \mathrm{d}t \exp[-i(\omega-\omega_{\mu 0}-\gamma_{\mu\mu}E_\lambda)t]\cdot \exp[G_\mu(t)-G_\mu(0)]\exp\left(-\frac{t}{\tau_\mu}\right) \quad (20)$$

where

$$\gamma_{\mu\nu} = \sum_m (c_m^\mu c_m^\nu)^2 \quad (21)$$

The time-dependent function $G_\mu(t)$ in Eq.(19) and Eq.(20) is given by

$$G_\mu(t) = \gamma_{\mu\mu}G(t) \quad (22)$$

$$G(t) = \int_0^\infty \mathrm{d}\omega\{(1+n(\omega))J(\omega)\exp(-i\omega t) + n(\omega)J(\omega)\exp(i\omega t)\} \quad (23)$$

where $n(\omega)$ is the mean number of vibrational quanta in equilibrium:

$$n(\omega) = \frac{1}{\exp(\beta\omega)-1} \quad (24)$$

τ_μ^{-1} is a decaying rate constant caused by population relaxation (*i.e.*, the T_1 process) [28],

$$\tau_\mu^{-1} = \frac{1}{2}\sum_\nu k_{\mu\to\nu} \quad (25)$$

3. Two-dimensional spectra

In the impulsive limit, the absorptive part of the 2D spectra can be calculated as the real part of the following sum of the double Fourier-Laplace transforms of the rephasing and nonrephasing response functions [21, 30],

$$S(\omega_3,t_2,\omega_1) = \mathrm{Re}\int_0^\infty\int_0^\infty \mathrm{d}t_1\mathrm{d}t_3\{\exp[i(\omega_1 t_1+\omega_3 t_3)]\cdot \tilde{R}_{\mathrm{nr}}(t_3,t_2,t_1) + \exp[i(-\omega_1 t_1+\omega_3 t_3)]\cdot \tilde{R}_{\mathrm{rp}}(t_3,t_2,t_1)\} \quad (26)$$

where the third-order response function can be calculated as [26, 30]:

$$\tilde{R}_{\mathrm{S}}(t_3,t_2,t_1) = \sum_{\mu\nu} W_\mu(t_3)G_{\mu\nu}(t_2)D_\nu(t_1) - \sum_\mu W_\mu(t_3)D_\mu(t_1) + R_{\mathrm{S}}(t_3,t_2,t_1) \quad (27)$$

where subscript S stands for the rephasing (rp) or nonrephasing (nr) signals. Here, $R(t_3,t_2,t_1)$ (we have dropped the S subscript for simplicity) is the coherence term and the latter two are population terms. The $R(t_3,t_2,t_1)$ term can be calculated as

$$R(t_3,t_2,t_1) = R_{\mathrm{I}}(t_3,t_2,t_1) + R_{\mathrm{II}}(t_3,t_2,t_1) + R_{\mathrm{III}}(t_3,t_2,t_1) \quad (28)$$

where the three terms R_{I}, R_{II}, and R_{III} denote contributions from the stimulated emission, ground state bleaching, and excited state absorption [26]. W and D are the window and doorway function, respectively. Detailed expressions of the R, W and D terms can be found in Refs.[26, 30]. $G_{\mu\nu}(t_2)$ in the second term is the Green function of the master equation for exciton-hopping between the exciton eigenstates, which is describe by the following equation:

$$\frac{\mathrm{d}}{\mathrm{d}t}G_{\mu\nu}(t) = \sum_{\alpha\neq\mu}[K_{\mu\alpha}G_{\alpha\nu}(t) - K_{\alpha\mu}G_{\mu\nu}(t)] \quad (29)$$

with the initial condition $G_{\mu\nu}(0)=\delta_{\mu\nu}$. After diagonalizing the rate constant matrix K, $G_{\mu\nu}(t)$ can be calculated as [30],

$$G_{\mu\nu}(t) = \sum_l \frac{Q_{\mu l}}{Q_{l\nu}}\exp(-\lambda_l t) \quad (30)$$

where Q is the matrix that diagonalizes K and λ_{ls} are the eigenvalues.

III. RESULTS

A. Model dimers

We first investigate the case of model dimers. The two two-level chromophores are assumed to have the same transition energies, $\epsilon_1=\epsilon_2=\epsilon$, and transition dipole moments, $\mu_1=\mu_2$. The electronic coupling between them is assumed to be $-J$, where $J>0$. This corresponds to a typical case of J-aggregate. The bath spectral density $J_m(\omega)$ is assumed to be the same for all molecules, and the Debye spectral density is used,

$$J(\omega) = \frac{\eta\gamma\omega}{\omega^2+\gamma^2} \quad (31)$$

Figure 1 shows the absorption line shapes calculated by the HEOM and modified Redfield method with different sets of parameters. Figure 1(a) compares the results at different temperatures T with $\eta=0.5J$ and $\gamma=0.3J$, Fig.1(b) shows the results for different system-bath coupling strengths η with $\beta J=1$ and $\gamma=0.3J$, and Fig.1(c) for different bath relaxation rate constants γ with $\beta J=1$ and $\eta=0.5J$. In general, the results from the modified Redfield method agree very well with those from the HEOM. We note that the small peak with the higher excitation energy is missing in the modified Redfield result. This is due to the fact that the higher

DOI:10.1063/1674-0068/28/cjcp1506126

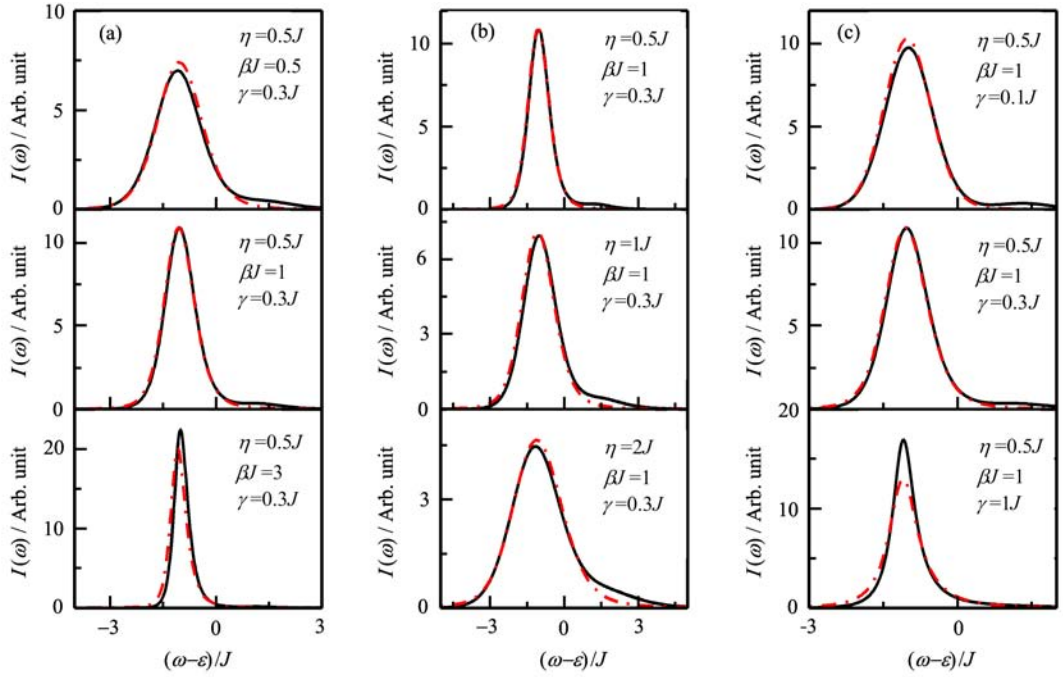

FIG. 1 Absorption line shapes of model dimer calculated with the HEOM (solid line) and modified Redfield (dash-dotted line) methods with different sets of parameters. (a) The results at different temperatures, (b) the results for different system-bath coupling strengths, and (c) the results for different bath relaxation rate constants.

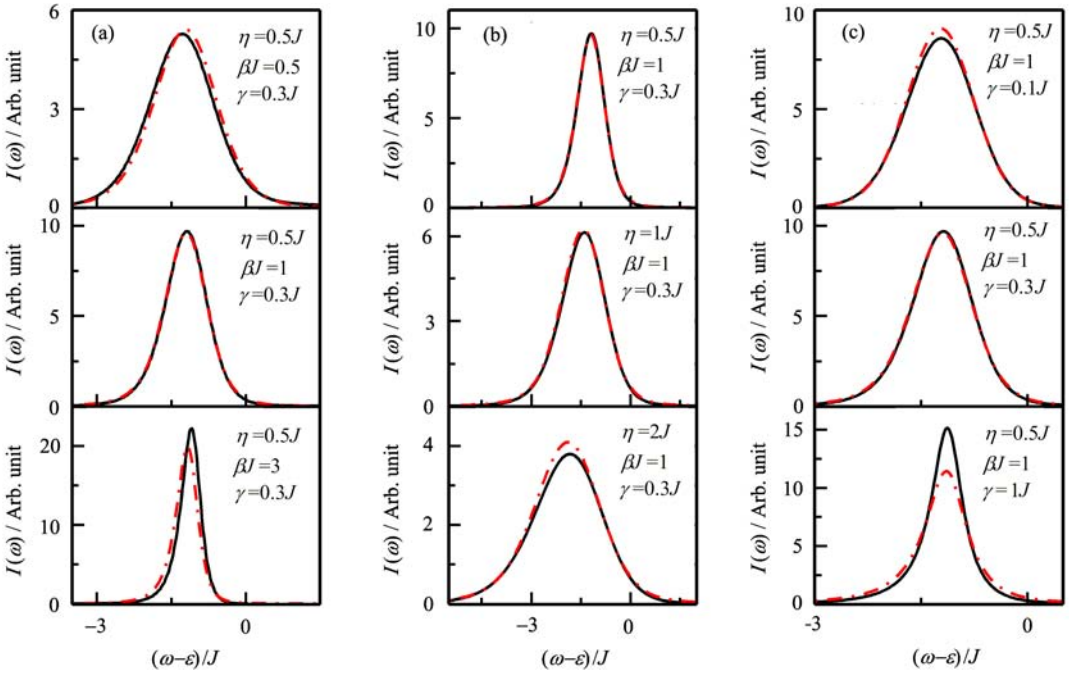

FIG. 2 Emission line shapes of model dimer calculated with the HEOM (solid line) and modified Redfield (dash-dotted line) methods with different sets of parameters for the emission line shapes. (a) The results at different temperatures, (b) the results for different system-bath coupling strengths, and (c) the results for different bath relaxation rate constants.

exciton state happens to carry zero oscillation strength for the symmetric dimer. Slightly larger deviations of the modified Redfield results are also observed for large intermolecular couplings and fast bath.

The emission line shapes of the model dimers calculated using the HEOM and modified Redfield methods are presented in Fig.2, with the same parameters as in Fig.1. Again, results from the modified Redfield

DOI:10.1063/1674-0068/28/cjcp1506126

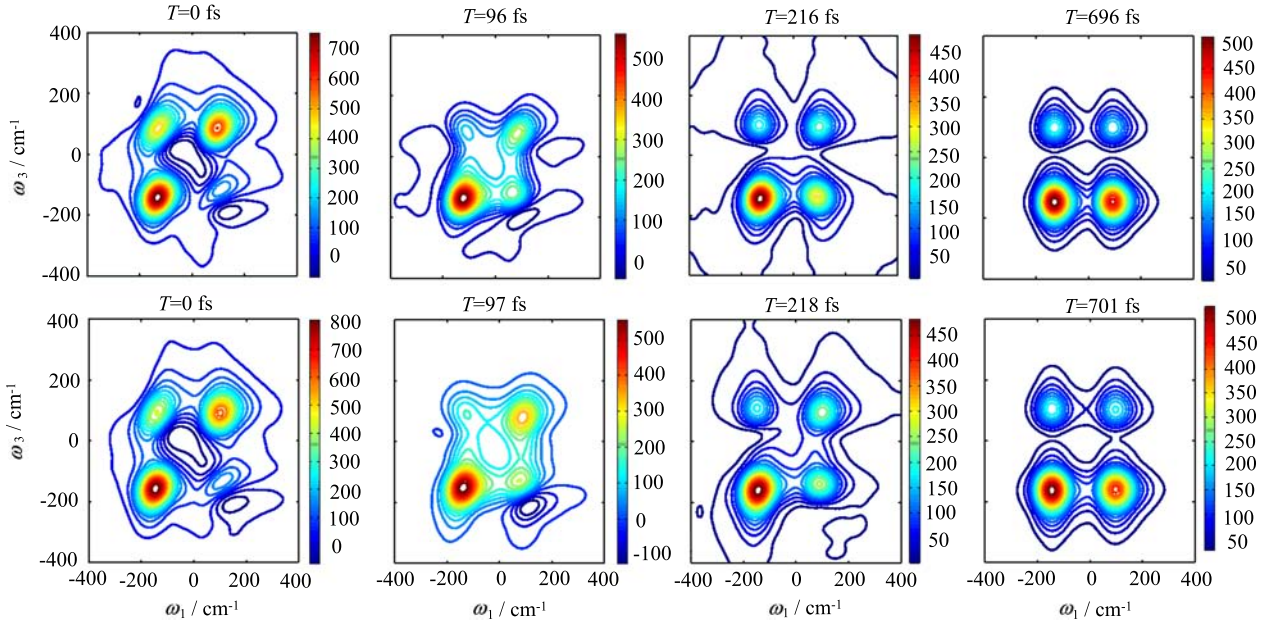

FIG. 3 2D spectra of the model dimer calculated with HEOM (lower) and modified Redfield (upper) methods, for the case without static disorder.

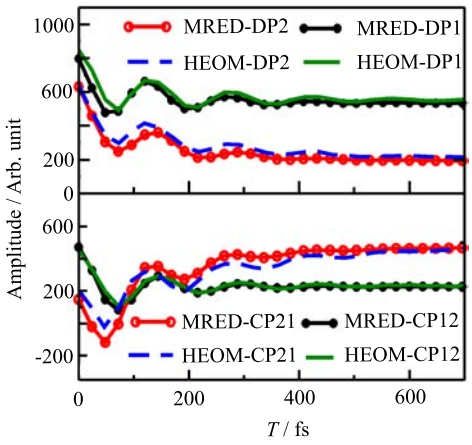

FIG. 4 Oscillatory patterns of the amplitudes of the four major peaks in the 2D electronic spectra of the model dimer without static disorder, calculated using the modified Redfield and HEOM methods.

method agree very well with those from the HEOM. Since the emission spectra are calculated from the equilibrium excited state, the small high energy peak in the absorption spectra does not appear in the emission spectra, and the agreement for emission line shapes are better than the absorption ones. We note this holds only for the special case of a J-aggregate, the situation may be different in other parameter regimes.

We then turn to the calculation of 2D spectra for model dimers. The case without static disorder is first investigated. The parameters used in the simulation are the same as in our previous paper using the HEOM method [21]: ϵ_1=−50 cm^{-1}, ϵ_2=50 cm^{-1}, J_{12}=100 cm^{-1}, γ^{-1}=100 fs, and η=120 cm^{-1} corresponding to a reorganization energy of 60 cm^{-1}. The transition dipoles of the two monomers are assumed to be perpendicular to each other, and the temperature is 77 K. Figure 3 shows the 2D spectra calculated using the modified Redfield and HEOM methods at different waiting time t_2=T. The shapes of the 2D spectra calculated from the two different methods are very similar.

We have also calculated the oscillatory patterns of the four major (two diagonal and two off-diagonal) peaks in the 2D spectra, which is presented in Fig.4, where DP1 and DP2 indicate the lower and higher diagonal peaks, CP12 and CP21 indicate the upper left and lower right off-diagonal peaks. We can see that the oscillatory patterns for all the four peaks from the modified Redfield method agree well with those from the numerically exact HEOM method. An interesting question is that, where the amplitude oscillations of the 2D peaks come from by using the modified Redfield calculations. Further investigation shows that the oscillations originate from the $R_{\rm I}$ and $R_{\rm III}$ terms, which are the excited stimulated emission (ESE) and the excited state absorption (ESA) contributions [26, 30]. From Eq.(30), it is clear that population transfer among exciton eigenstates would not lead to oscillatory signals since only rate dynamics is involved for energy hopping between exciton eigenstates. So the oscillatory patterns originate from simultaneous excitation of different exciton states, rather than coherent energy transfer between different exciton states.

Figure 5 shows the 2D spectra calculated using the modified Redfield and HEOM methods, in the presence of static disorder. The static disorder is assumed to be

DOI:10.1063/1674-0068/28/cjcp1506126

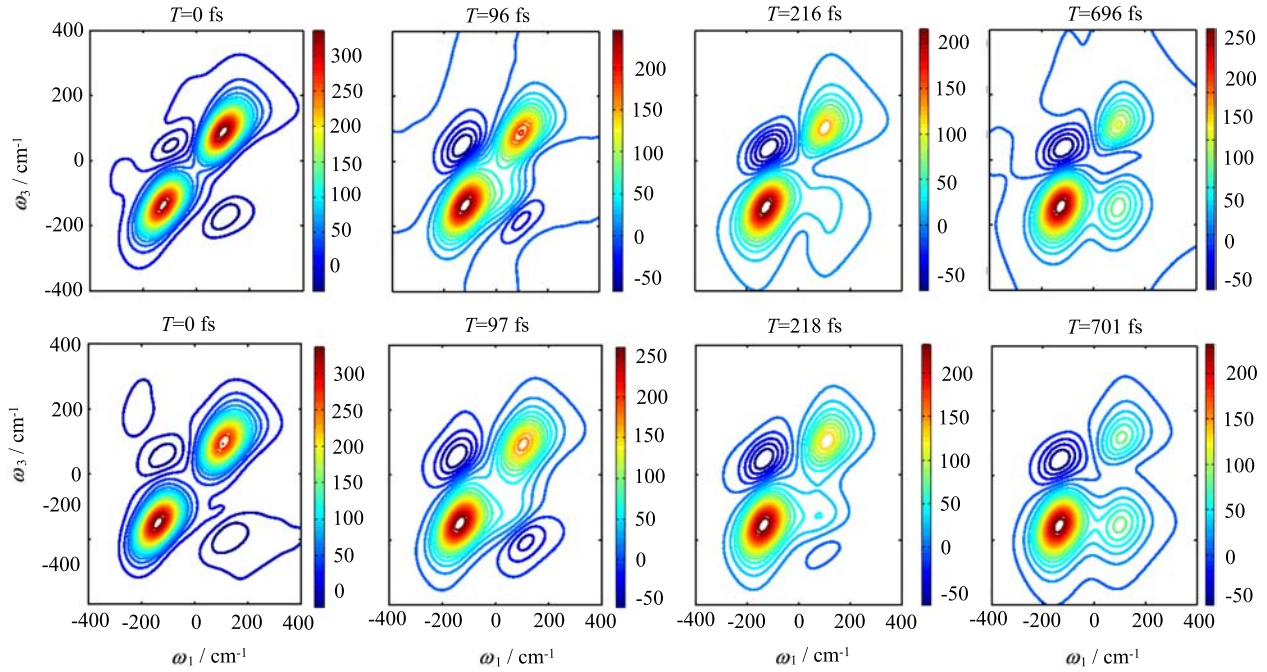

FIG. 5 2D spectra of the model dimer calculated with HEOM (lower) and modified Redfield (upper) methods in the presence of static disorder.

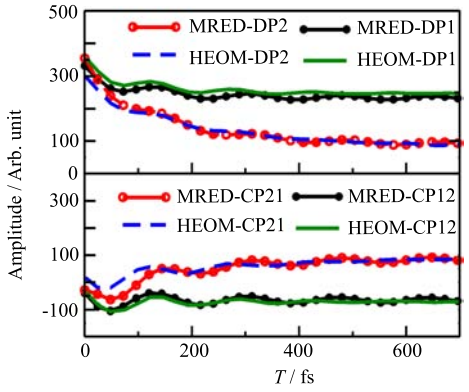

FIG. 6 Oscillatory patterns of the amplitudes of the four major peaks in the 2D electronic spectra of the model dimer in the presence of static disorder calculated using the modified Redfield and HEOM methods,

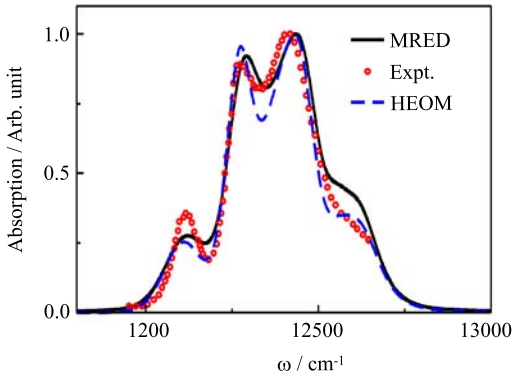

FIG. 7 Simulated absorption line shape of the FMO complex from *C. tepidum*, using the modified Redfield and HEOM methods. The open circles are experimental results from Ref.[30].

independent for the two sites, and described by a Gaussian distribution with a full width at half maximum (FWHM) of 100 cm^{-1}. Similar to the results without static disorder, the shapes of the 2D spectra calculated from the modified Redfield method agree well with the HEOM results. Oscillations of the four major peaks from modified Redfield method presented in Fig.6 also agree well with the HEOM results.

B. The FMO complex

In this subsection, we present the simulation results for the Fenna-Matthews-Olson (FMO) complex, which has served as an important model system to study the effect of coherent energy transfer in both experimental [8, 9, 11, 47] and theoretical studies [22, 44, 45, 48]. The absorption and 2D spectra has been studied using the modified Redfield method by Cho *et al.* previously [30]. To compare with the numerical exact HEOM method, we employ the Debye spectral density which has been used in our previous work [22], rather than the Ohmic spectral density with exponential cut-off in Ref.[30]. We employ the model Hamiltonian for the FMO complex of *C. tepidum* from Refs.[22, 30]. For the parameters in the spectral density, the reorganization energy is assumed to be 35 cm^{-1}, the relaxation time constant is

DOI:10.1063/1674-0068/28/cjcp1506126

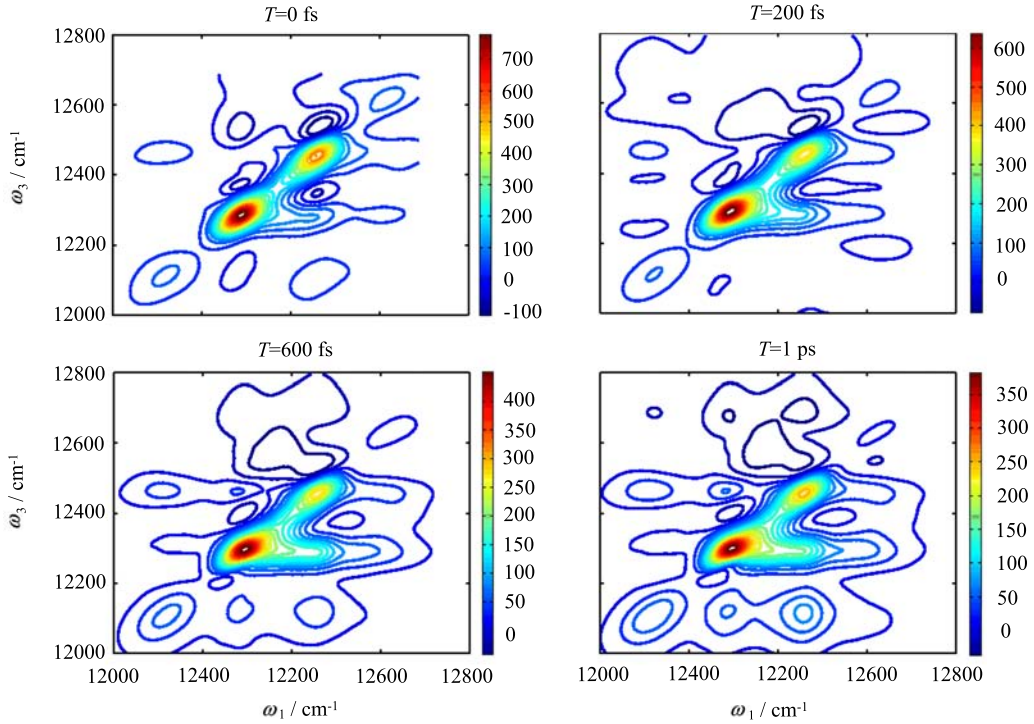

FIG. 8 Simulated 2D spectra of the FMO complex from *C. tepidum* by the modified Redfield method. The waiting times are 0, 200, 600 fs, and 1 ps, respectively.

γ^{-1}=100 fs, and the FWHM of the static disorder is assumed to be 100 cm^{-1}. Both of the linear and nonlinear spectra were obtained by averaging over 1000 samples.

Figure 7 shows the absorption spectra calculated by modified Redfield method, compared with the HEOM and experimental results. We can see that the modified Redfield result agrees well with the HEOM result with some small deviations. Both the HEOM and modified Redfield methods give broader line shape than the experiment at the location of the first exciton peak, which indicates that the static and dynamics disorder used for pigment 3 (which is the main component of the first exciton state) is probably too large.

The 2D spectra calculated using the modified Redfield method at T=0, 200, 600 fs, and 1 ps are shown in Fig.8, it can be seen that they agree well with the numerical exact results in Ref.[22].

IV. CONCLUSION

In the past years, the modified Redfield method has become a popular approach to calculate linear and nonlinear spectroscopic signals due to its efficiency and relative high accuracy. Recently, some of the approximations employed in its derivation have been questioned in the intermediate coupling regime [7, 19, 33–36]. In this work, we test the validity of the modified Redfield method in simulations of linear and nonlinear spectroscopic signals in photosynthetic light harvesting complexes, by comparing with the numerically exact HEOM method. In the case of model dimers, the absorption and emission line shapes are first calculated and the results from the two approaches agree very well, although noticeable deviations can be observed. The modified Redfield method also give good results in calculations of the 2D spectra of model dimers, either with or without static disorder. Especially, the modified Redfield method also reproduces well the oscillatory patterns of the diagonal and off-diagonal peaks in the 2D spectral when there is strong intermolecular coupling. This indicates that the quantum beats in the 2D spectra originate from the quantum coherence caused by simultaneous excitation of different exciton states, rather than coherent population transfer between them. In simulations of the FMO complex, although there are also some noticeable differences in the absorption line shape, the main features of the absorption line shape and 2D spectra calculated using the modified Redfield method agree well with the HEOM simulations and the experiment. Thus, we conclude that the modified Redfield method is a valid approach in calculating spectral signals in a wide range of parameters. Further investigations of its limits and possible improvements over the perturbative and Markovian approximations will be left for future works.

V. ACKNOWLEDGMENTS

This work was supported by the National Natural Science Foundation of China (No.21290194), the

DOI:10.1063/1674-0068/28/cjcp1506126

National Basic Research Program (No.2011CB808502 and No.2013CB933501), and the Strategic Priority Research Program of Chinese Academy of Sciences (No.XDB12020300).

[1] T. Kobayashi, *J-Aggregates*, Singapore: World Scientific, (1996).
[2] H. van Amerongen, L.Valkunas, and R. van Grondelle, *Photosythetic Exictons*, Singapore: World Scientific, (2000).
[3] R. van Grondelle and V. I. Novoderezhkin, Phys. Chem. Chem. Phys. **8**, 793 (2006).
[4] S. K. Saikin, A. Eisfeld, S. Valleau, and A. Aspuru-Guzik, Nanophotonics **2**, 21 (2013).
[5] S. Mukamel, *Principles of Nonlinear Optical Spectroscopy,* New York: Oxford, (1995).
[6] S. Mukamel, Y. Tanimura, and P. Hamm, Acc. Chem. Res. **42**, 1207 (2009).
[7] Y. C. Cheng and G. R. Fleming, Annu. Rev. Phys. Chem. **60**, 241 (2009).
[8] T. Brixner, J. Stenger, H. M. Vaswani, M. Cho, R. E. Blankenship, and G. R. Fleming, Nature **434**, 625 (2005).
[9] G. S. Engel, T. R. Calhoun, E. L. Read, T. K. Ahn, T. Mancal, Y. C. Cheng, R. E. Blankenship, and G. R. Fleming, Nature **446**, 782 (2007).
[10] E. Collini, C. Y. Wong, K. E. Wilk, P. M. G. Curmi, P. Brumer, and G. D. Scholes, Nature **463**, 644 (2010).
[11] G. Panitchayangkoon, D. Hayes, K. A. Fransted, J. R. Caram, E. Harel, J. Wen, R. E. Blankenship, and G. S. Engel, Proc. Natl. Acad. Sci. USA **107**, 12766 (2010).
[12] S. Westenhoff, D. Palecek, P. Edlund, P. Smith, and D. Zigmantas, J. Am. Chem. Soc. **134**, 16484 (2012).
[13] F. D. Fuller, J. Pan, A. Gelzinis, V. Butkus, S. S. Senlik, D. E. Wilcox, C. F. Yocum, L. Valkunas, D. Abramavicius, and J. P. Ogilvie, Nat. Chem. **6**, 706 (2014).
[14] E. Romero, R. Augulis, V. I. Novoderezhkin, M. Ferretti, J. Thieme, D. Zigmantas, and R. van Grondelle, Nat. Phys. **10**, 676 (2014).
[15] V. May and O. Kühn, *Charge and Energy Transfer Dynamics in Molecular Systems*, 3rd Edn., Weinheim: Wiley-VCH, (2011).
[16] T. Renger, V. May, and O. Kühn, Phys. Rep. **343**, 137 (2001).
[17] M. Yang and G. R. Fleming, Chem. Phys. **282**, 163 (2002).
[18] Y. J. Yan and R. X. Xu, Annu. Rev. Phys. Chem. **56**, 187 (2005).
[19] A. Ishizaki and G. R. Fleming, J. Chem. Phys. **130**, 234110 (2009).
[20] L. P. Chen, R. H. Zheng, Q. Shi, and Y. J. Yan, J. Chem. Phys. **131**, 094502 (2009).
[21] L. P. Chen, R. H. Zheng, Q. Shi, and Y. J. Yan, J. Chem. Phys. **132**, 024505 (2010).
[22] L. P. Chen, R. H. Zheng, Y. Y. Jing, and Q. Shi, J. Chem. Phys. **134**, 194508 (2011).
[23] Y. Y. Jing, L. P. Chen, S. M. Bai, and Q. Shi, J. Chem. Phys. **138**, 045101 (2013).
[24] A. G. Redfield, IBM J. Res. **1**, 19 (1957).
[25] W. T. Pollard, A. K. Felts, and R. A. Friesner, Adv. Chem. Phys. **93**, 77 (1996).
[26] W. M. Zhang, T. Meier, V. Chernyak, and S. Mukamel, J. Chem. Phys. **108**, 7763 (1998).
[27] K. Ohta, M. Yang, and G. R. Fleming, J. Chem. Phys. **115**, 7609 (2001).
[28] T. Renger and R. A. Marcus, J. Chem. Phys. **116**, 9997 (2002).
[29] V. I. Novoderezhkin, M. A. Palacios, H. van Amerongen, and R. van Grondelle, J. Phys. Chem. B **108**, 10363 (2004).
[30] M. Cho, H. M. Vaswani, T. Brixner, J. Stenger, and G. R. Fleming, J. Phys. Chem. B **109**, 10542 (2005).
[31] M. Schröder, M. Schreiber, and U. Kleinekathöfer, J. Chem. Phys. **126**, 114102 (2007).
[32] M. Cho, Chem. Rev. **108**, 1331 (2008).
[33] Y. H. Hwang-Fu, W. Chen, and Y. C. Cheng, Chem. Phys. **447**, 46 (2015).
[34] Y. Chang and Y. C. Cheng, J. Chem. Phys. **142**, 034109 (2015).
[35] T. C. Dinh and T. Renger, J. Chem. Phys. **142**, 034104 (2015).
[36] A. Gelzinis, D. Abramavicius, and L. Valkunas, J. Chem. Phys. **142**, 154107 (2015).
[37] Y. Tanimura and R. K. Kubo, J. Phys. Soc. Jpn. **58**, 101 (1989).
[38] Y. Tanimura, J. Phys. Soc. Jpn. **75**, 082001 (2006).
[39] Y. Yan, F. Yang, Y. Liu, and J. Shao, Chem. Phys. Lett. **395**, 216 (2004).
[40] R. X. Xu, P. Cui, X. Q. Li, Y. Mo, and Y. J. Yan, J. Chem. Phys. **122**, 041103 (2005).
[41] A. Ishizaki and Y. Tanimura, J. Phys. Soc. Jpn. **74**, 3131 (2005).
[42] Q. Shi, L. P. Chen, G. J. Nan, R. X. Xu, and Y. J. Yan, J. Chem. Phys. **130**, 084105 (2009).
[43] A. Ishizaki and G. R. Fleming, J. Chem. Phys. **130**, 234111 (2009).
[44] A. Ishizaki and G. R. Fleming, Proc. Natl. Acad. Sci. USA **106**, 17255 (2009).
[45] J. Zhu, S. Kais, P. Rebentrost, and A. Aspuru-Guzik, J. Phys. Chem. B **115**, 1531 (2011).
[46] T. Renger and R. Marcus, J. Phys. Chem. A **107**, 8404 (2003).
[47] S. Savikhin, D. R. Buck, and W. S. Struve, Chem. Phys. **223**, 303 (1997).
[48] S. M. Bai, K. Song, and Q. Shi, J. Phys. Chem. Lett. **6**, 1954 (2015).

DOI:10.1063/1674-0068/28/cjcp1506126